A comparison of two global datasets of extreme sea levels and resulting flood exposure

Muis, S.; Verlaan, Martin; Nicholls, Robert J.; Brown, Sally; Hinkel, Jochen; Lincke, Daniel; Vafeidis, Athanasios T.; Scussolini, Paolo; Winsemius, Hessel; Ward, Philip J.

DOI
10.1002/2016EF000430

Publication date
2017

Document Version
Final published version

Published in
Earth's Future

Citation (APA)
Muis, S., Verlaan, M., Nicholls, R. J., Brown, S., Hinkel, J., Lincke, D., Vafeidis, A. T., Scussolini, P., Winsemius, H., & Ward, P. J. (2017). A comparison of two global datasets of extreme sea levels and resulting flood exposure. *Earth's Future*, *5*(4), 379-392. https://doi.org/10.1002/2016EF000430

AGU PUBLICATIONS

Earth's Future

RESEARCH ARTICLE
10.1002/2016EF000430

A comparison of two global datasets of extreme sea levels and resulting flood exposure

Sanne Muis[1], Martin Verlaan[2,3], Robert J. Nicholls[4,5], Sally Brown[4,5], Jochen Hinkel[6,7], Daniel Lincke[6], Athanasios T. Vafeidis[8], Paolo Scussolini[1], Hessel C. Winsemius[2], and Philip J. Ward[1]

[1]Institute for Environmental Studies (IVM), Vrije Universiteit Amsterdam, Amsterdam, The Netherlands, [2]Deltares, Delft, The Netherlands, [3]Mathematical Physics, Electrical Engineering, Mathematics and Computer Science (EEMCS), Delft Technical University, Delft, The Netherlands, [4]Faculty of Engineering and the Environment, University of Southampton, Southampton, UK, [5]Tyndall Centre for Climate Change Research, Southampton, UK, [6]Global Climate Forum, Department of Adaptation and Social Learning, Berlin, Germany, [7]Division of Resource Economics, Albrecht Daniel Thaer-Institute and Berlin Workshop in Institutional Analysis of Social-Ecological Systems (WINS), Humboldt-University, Berlin, Germany, [8]Institute of Geography, Christian Albrechts University, Kiel, Germany

Abstract Estimating the current risk of coastal flooding requires adequate information on extreme sea levels. For over a decade, the only global data available was the DINAS-COAST Extreme Sea Levels (DCESL) dataset, which applies a static approximation to estimate extreme sea levels. Recently, a dynamically derived dataset was developed: the Global Tide and Surge Reanalysis (GTSR) dataset. Here, we compare the two datasets. The differences between DCESL and GTSR are generally larger than the confidence intervals of GTSR. Compared to observed extremes, DCESL generally overestimates extremes with a mean bias of 0.6 m. With a mean bias of −0.2 m GTSR generally underestimates extremes, particularly in the tropics. The Dynamic Interactive Vulnerability Assessment model is applied to calculate the present-day flood exposure in terms of the land area and the population below the 1 in 100-year sea levels. Global exposed population is 28% lower when based on GTSR instead of DCESL. Considering the limited data available at the time, DCESL provides a good estimate of the spatial variation in extremes around the world. However, GTSR allows for an improved assessment of the impacts of coastal floods, including confidence bounds. We further improve the assessment of coastal impacts by correcting for the conflicting vertical datum of sea-level extremes and land elevation, which has not been accounted for in previous global assessments. Converting the extreme sea levels to the same vertical reference used for the elevation data is shown to be a critical step resulting in 39–59% higher estimate of population exposure.

Key Points:
- An earlier global dataset that applies a static approach overestimates sea-level extremes, but provides a good estimate of spatial variation
- A new dynamically derived global dataset of sea-level extremes provides an improved basis for the assessment of the impacts of coastal flooding
- Correcting for the conflicting vertical datum of sea-level extremes and global elevation results in large changes in flood exposure

Supporting Information:
- Supporting Information S1

Corresponding author:
S. Muis, sanne.muis@vu.nl

Citation:
Muis, S., M. Verlaan, R. J. Nicholls, S. Brown, J. Hinkel, D. Lincke, A. T. Vafeidis, P. Scussolini, H. C. Winsemius, and P. J. Ward (2017), A comparison of two global datasets of extreme sea levels and resulting flood exposure, *Earth's Future*, *5*, 379–392, doi:10.1002/2016EF000430.

Received 18 AUG 2016
Accepted 12 MAR 2017
Accepted article online 17 MAR 2017
Published online 3 APR 2017

1. Introduction

Storm surges are a major cause of coastal flooding, and can lead to devastating societal impacts [*Kron*, 2013]. There has been an upward trend in global flood exposure during recent decades [*Jongman et al.*, 2012]. Without adaptation, risks are projected to increase further due to population and economic growth, migration towards the coast, subsidence, and climate change [*Hallegatte et al.*, 2013; *Hinkel et al.*, 2014; *Güneralp et al.*, 2015]. In particular, sea-level rise will increase the frequency of extreme sea levels and hence the potential severity of coastal flooding [*Nicholls and Cazenave*, 2010]. Based on projected sea level rise of 25–123 cm by 2100, with respect to 1985–2005, a range of population projections, and assuming constant protection levels, the population experiencing coastal flooding on average per year is estimated to reach 0.2–4.6% [*Hinkel et al.*, 2014]. Widespread adaptation will be required to prevent such large impacts. To support decisions on adaptation, we need global models that can provide large-scale assessments of coastal risk [*Ward et al.*, 2015].

The Global Vulnerability Assessment (GVA) provided the first global estimates for extreme sea levels per country, using a static approximation of storm surge conditions and mean high tide. In 2004, the DINAS-COAST project improved the GVA extremes and produced the DINAS-COAST Extreme Sea Levels (DCESL) dataset. DCESL applies the same method as the GVA, but at a much higher spatial resolution: instead of estimates per country, extremes are provided for 12,148 segments around the world's coasts, excluding Antarctica [*McFadden et al.*, 2007; *Vafeidis et al.*, 2008; *Hinkel and Klein*, 2009]. For over a decade,

DCESL has been the only global dataset of extreme sea levels. Several continental to global-scale studies have applied DCESL to assess coastal flood risk using the Dynamic Interactive Vulnerability Assessment (DIVA) model [*Nicholls et al.*, 2010; *Hinkel et al.*, 2011, 2014; *Brown et al.*, 2013], and other impact models [*Sugiyama et al.*, 2008; *Ward et al.*, 2010; *Jongman et al.*, 2012; *Hallegatte et al.*, 2013; *Muis et al.*, 2015]. As such, the DCESL dataset has enabled important insight into the dynamics of coastal flood risk and has helped to identify which coastal areas may experience the highest increases in risk due to sea-level rise, assuming extreme sea levels simply shift with increasing long-term sea-level rise.

At the regional-scale, hydrodynamic modeling is the state-of-the-art to assess coastal flood hazard, but computational costs have hampered global-scale applications. Recent advances in numerical methodologies (i.e., use of *unstructured grids*) and high-performance computing have enabled the development of a dynamically derived dataset of sea-level extremes: the Global Tide and Surge Reanalysis (GTSR) dataset [*Muis et al.*, 2016]. GTSR presents extreme sea levels for the world's coastline at the resolution of the DIVA coastal segments.

To assess the advancement of GTSR over DCESL, we evaluate the differences between the two datasets by comparing them against each other and against observed extreme sea levels to quantify the respective biases. Further, we present a comparison of present-day coastal impacts by applying the DIVA model to calculate flood exposure based on the 1 in 100-year sea levels from DCESL and GTSR. Past studies have not accounted for the difference in vertical datum of extreme sea levels and global land elevation. In this study, we also investigate the effects of converting the vertical datum of the sea-level extremes to the one that is used for the land elevation.

2. Methods

2.1. Modeled Extreme Sea Levels

The DCESL and GTSR extreme sea levels for different return periods (referred to as "extremes" in the remainder of this article) are composed of four terms: mean sea level relative to reference level, astronomical tide, atmospheric pressure effects (i.e., inverse barometer effect), and wind effects (i.e., wind set-up, the pilling up of the sea level due to the force of wind). Nonlinear interaction effects may increase the water level further, but these effects are not included in either of the datasets analyzed here. Also, the effects of waves are not considered, while wave run-up and wave set-up can also contribute to extremes. The main difference between DCESL and GTSR is that DCESL calculates extremes statically, while GTSR dynamically. In the following, we outline details of these two approaches.

2.1.1. DCESL Extremes

The DCESL database contains estimates of extreme sea levels with return periods of 1, 10, 100, and 1,000 years for each of the 12,148 coastal segments of the DIVA model [*McFadden et al.*, 2007]. The segments have a variable length (average 70 km) depending on physical and socio-economic characteristics [*Vafeidis et al.*, 2008]. Sea-levels extremes are reconstructed by:

$$H\left(f\right) = H_{\mathrm{mh}} + H_{\mathrm{p}}\left(f\right) + H_{\mathrm{s}}\left(f\right) \tag{1}$$

where H is the total extreme water level with frequency of occurrence f, H_{mh} is the mean high-tide level, H_{p} is the component of the barometric pressure induced by a storm with frequency of occurrence f, and H_{s} is the wind set-up by a storm with frequency of occurrence f. The mean high-tide level is based on harmonic constants produced with the program XTIDE (www.flaterco.com/xtide), based on the database of the United Kingdom Hydrographic Office containing observations from ports around the world. Values were derived from the LOICZ database [*Maxwell and Buddemeier*, 2002] and were averaged over the length of each coastline segment. The barometric term is assumed to be equal to 0.1, 0.2, 0.3, and 0.4 m for return periods of 1, 10, 100, and 1,000 years, respectively.

The wind set-up is calculated using a simplification of the shallow water equations, which assumes equilibrium with constant wind speed and an infinitely long straight beach coast with a uniform bottom slope. The wind set-up for segment i, which is on a line perpendicular to the coastal segment, is given by *Weenink* [1958]:

$$H_{\mathrm{s},i}\left(f\right) = H_{\mathrm{s},i-1}\left(f\right) + C\frac{u_{\mathrm{w}}^2}{gb_i}\ln\left(\frac{h_i + H_{\mathrm{s},i-1}\left(f\right)}{h_{i-1} + H_{\mathrm{s},i-1}\left(f\right)}\right) \tag{2}$$

where C is a constant, b_i (−) is the sea bed slope, u_w is the daily averaged wind speed at a height of 10 m perpendicular to the coast (m s^{-1}), g is the gravitational constant (m s^{-2}), and h is the depth with respect to mean sea level (m). At deep water the wind effect is assumed to be negligible ($H_{s,0} = 0$). For DCESL, only one section ($i = 1$) was used to calculate the surge level near the coast ($H_{s,1}$). To the bathymetry into account, the average sea bed slope for each DIVA segment is calculated over a distance of 50 km offshore using ETOPO2 data [*National Geophysical Data Center (NGDC)*, 2001]. The GVA estimates by *Hoozemans et al.* [1993] were developed prior to global climate reanalysis datasets. Therefore, wind speeds were estimated from wave observations (the reverse approach to most coastal analyses). Wave height of storms with short return periods (<10 years) are derived from *Global Wave Statistics* [*Hogben et al.*, 1986] and are extrapolated to longer return periods using a log-linear distribution [*Hoozemans et al.*, 1993]. Finally, these wave heights were converted to wind speeds (u_w) based on *Hurdle and Stive* [1989]. With the same wind speed, the wind set-up is higher for flat shallow coastal areas and lower for steep, deep coastal areas.

2.1.2. GTSR Extremes

GTSR is the first global dataset of extreme sea levels based on hydrodynamic modeling [*Muis et al.*, 2016]. GTSR is based on two global models: the Global Tide and Surge Model (GTSM) to simulate storm surges [*Verlaan et al.*, 2015], and the Finite Element Solution (FES2012) to simulate tides [*Carrere et al.*, 2012]. By forcing GTSM with 6 hourly meteorological fields from the ERA-Interim climate reanalysis [*Dee et al.*, 2011], *Muis et al.* [2016] simulated surge levels for the period 1979–2014. The surge levels were added to the tidal levels to construct time series of total sea levels, with a temporal resolution of 10 min. Tides are modeled separately because at this stage the model performance of FES is better than GTSM [*Muis et al.*, 2016]. Extreme sea levels for nine return periods (2, 5, 10, 25, 50, 100, 250, 500, and 1,000 years) were estimated by fitting a Gumbel distribution to the annual maxima [*Gumbel*, 1941]. The 5 and 95% confidence intervals of the parameterized extreme value distribution were also obtained. The GTSR data are available for each of the centroids of the DIVA segments as well as for each location of the tide gauge stations in the dataset of the University of Hawaii Sea Level Center (UHSLC).

2.2. Evaluation Criteria to Assess the Performance of the Two Datasets

We evaluate the performance of DCESL and GTSR against hourly sea levels over the period 1980–2012 from 472 observation stations from the archive of UHSLC (http://uhslc.soest.hawaii.edu). All observations were quality-checked by tidal analysis and corrected for any trend [*Muis et al.*, 2016]. We fit a Gumbel extreme value distribution to the observed annual maxima to obtain extreme sea levels, including 5 and 95% confidence intervals, with return periods of 10, 100, and 1,000 years. To obtain reliable estimates, return periods of 10 years are calculated only for 301 out of 472 stations having more than 10 years of data. Return periods of 100 and 1,000 years are calculated only for 144 stations having more than 25 years of data.

Multiple criteria are used to evaluate the performance of the DCESL and GTSR extremes. All criteria evaluate the difference between the modeled and observed extremes. We use the overlapping period from the modeled and observed sea levels for the extreme value statistics, and evaluate each return period separately. The accuracy of the extremes is evaluated in terms of the mean bias (i.e., systematic deviation, thus, the average over- or underestimation) and the mean absolute error (i.e., average magnitude of the deviations) between the modeled and observed extremes. We also assess the reliability of the datasets by calculating the hit rate, which evaluates how many instances of the modeled extremes fall within the 5 and 95% confidence bounds of the observed extremes. The GTSR extremes also contain 5 and 95% confidence bounds. Hence, for GTSR we also count the instances where there is an overlap between the confidence bounds of the modeled extremes and the observed extremes.

2.3. Modeling Flood Exposure

We apply the flood module of the DIVA model (version DIVA-mf 1.2) [*Hinkel et al.*, 2014] to assess how differences in sea-level extremes between DCESL and GTSR translate into differences in exposure to coastal flooding. Flood exposure is calculated individually for each of the 12,148 coastal segments and then aggregated to country scale. Specifically, we compare results using the following two model output parameters, described in *Hinkel et al.* [2014]:

1. *Exposed area* in terms of the size of the potential floodplain lying below the sea level with a return period of 100 years. This is computed by using the Shuttle Radar Topography Mission (SRTM) global

elevation dataset [*Jarvis et al.*, 2008] and linearly interpolated between elevation increments for each coastal segment assuming no flood defenses, hydrological connectivity, and planar flood levels.

2. *Exposed population* in terms of the number of people living below the sea level with a return period of 100 years. The population data is derived from the Global Rural–Urban Mapping Project (GRUMP) [*Center for International Earth Science Information Network (CIESIN) et al.,* 2011], and extrapolated to the year 2015.

The DCESL and GTSR extremes are both use mean sea level as vertical datum, whereas SRTM elevation is referenced to the EGM96 geoid [*Farr and Kobrick*, 2001]. There can be an offset of up to 1.5 m between mean sea level and the geoid. This is due to the dynamic sea surface of the ocean [*Schaeffer et al.*, 2012], and largely determined by ocean currents. For inundation modeling, it is essential that the sea-level extremes and land elevation have the same vertical datum. To convert the vertical datum of the DCESL and GTSR extremes from mean sea level to the EGM96 geoid, we use to mean dynamic ocean topography (MDT). The MDT is the difference between the mean sea surface and the geoid. We use an estimate of the MDT by *Rio et al.* [2014] (Figure S1), Supporting Information, who calculated the MDT by combining geodetic data (i.e., altimetric mean sea surface over the period 1993–2012 and an accurate geoid) with in situ data (i.e., temperature and salinity of seawater, current velocity, etc.).

3. Results and Discussion

3.1. Intercomparison of the DCESL and GTSR Extremes

For a return period of 100 years, the DCESL and GTSR extremes show the same geographical pattern of regions with high and low sea levels (Figures 1a and 1b). For example, extremes are low in the Mediterranean Sea, whereas extremes are high in the Hudson Strait. There are however large absolute differences between DCESL and GTSR with the largest differences (>2.5 m) along the coastline of northeast Russia (Figure 1c). The smallest differences (<1.0 m) are found around northern Europe, Greenland, and the west coast of South America. The largest difference occurs in regions where the coastal segments are quite long. Hence, the GTSR estimate for the centroid of the segment may be not representative. Figure 1d shows that the 1 in 100-year DCESL extremes are within the confidence bounds of the GTSR extremes for only 5% of the coastal segments. Hence, the differences between the two datasets are generally larger than the confidence bounds of the GTSR extreme values distribution. Results for other return periods are similar (not shown).

3.2. Accuracy of the DCESL and GTSR Extremes

3.2.1. Average Performance Across All Observation Stations

Across all observation stations, DCESL systematically overestimates extreme sea levels, particularly for the longer return periods (Table 1). For the 1 in 100-year extremes, the mean bias is 0.55 m and the mean absolute error is 0.64 m. In contrast, GTSR underestimates extreme sea levels, although with a much smaller bias and absolute error, of −0.19 and 0.23 m, respectively. Across all return periods, the mean bias and mean absolute error for GTSR are between 58 and 70% lower than those for DCESL. Also, the performance of GTSR is more regular over the different return periods. Figure S2 shows scatter plots for the DCESL and GTSR extremes against observed extremes. For a return period of 100 tear, the correlation coefficient between GTSR extremes and observed extremes is 0.84, compared to 0.70 for the DCESL extremes.

For both dataset, the hit rate indicates a better performance with longer return periods (Table 1). This is mainly caused by wider confidences bounds for longer return periods. For the return period of 10 years, GTSR has a hit rate of 21%, compared to 8% for the DCESL extremes. With the hit rate ranging from 19 to 26%, the hit rate does not indicate a large difference in performance for DCESL and GTSR for return period of 100 and 1,000 years. However, if we include the confidence interval of GTSR, the hit rate for GTSR increases to 32–40% (Table 1). Hence, an additional improvement of GTSR over DCESL is the use of extreme value statistics, which allows to provide confidence intervals that show a larger uncertainty for longer return periods. Overall, the GTSR extremes are a large improvement as the applied hydrodynamic approach provides much more accurate extremes than the static DCESL approach.

3.2.2. Regional Variation in Performance Across All Observation Stations

The relatively high standard deviations of the mean biases and mean absolute errors indicate a large variability across the observation stations (Table 1). This is also illustrated in Figure 2, which shows the model

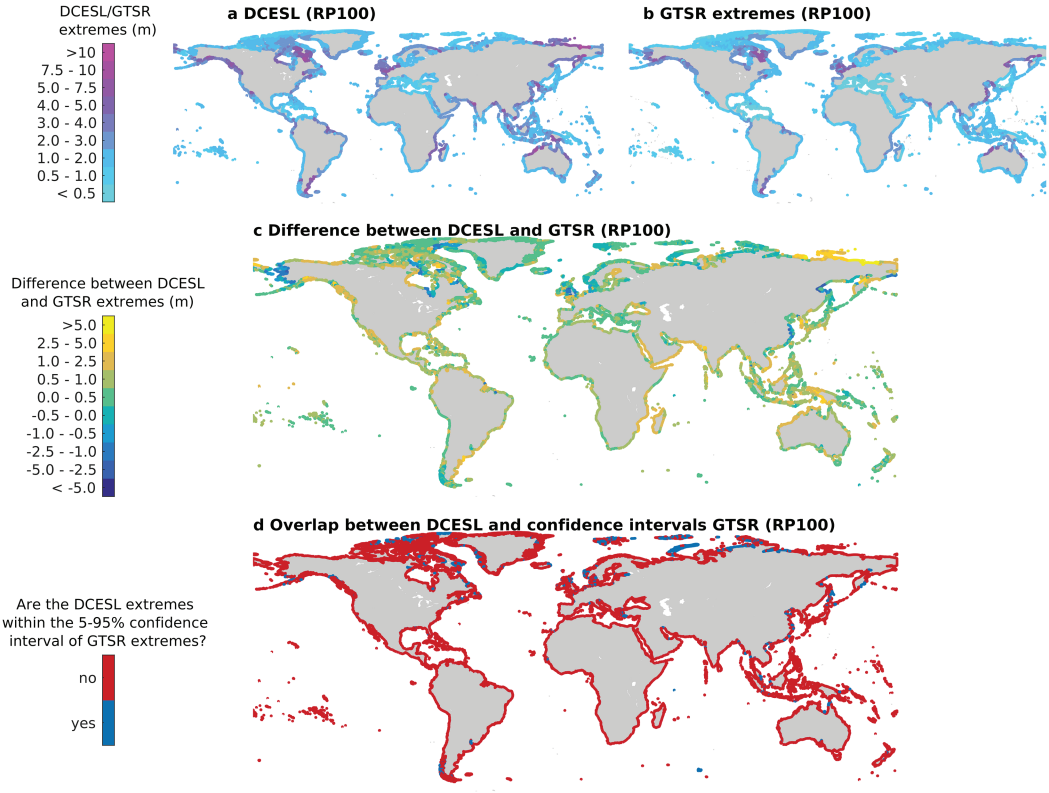

Figure 1. Maps showing (the differences between) the DINAS-COAST Extreme Sea Levels (DCESL) and Global Tide and Surge Reanalysis (GTSR) extremes with a return period of 100 years: (a) the height of DCESL sea level with a return period of 100 years relative to mean sea level; (b) the height of GTSR sea level with a return period of 100 years relative to mean sea level; (c) the difference between DCESL and GTSR. A positive value (orange to red colors) indicate that the DCESL extremes are larger than those in GTSR; and (d) whether the DCESL extremes are within the 5 and 95% confidence bounds of the fitted Gumbel distribution of the GTSR extremes.

bias for each station for 1 in 10-year extreme sea levels. Figure S3 shows the results for the return periods of 100 and 1,000 years. The bias of DCESL is particularly high (>1 m) along the coastlines of North America, the northwest of Australia, and the south of Asia. DCESL shows a better agreement with observations (bias <0.25 m) along the European, western South American, and South African coastline. The bias of GTSR is generally below 0.5 m, although there are some locations where the bias is larger than 1 m. At those locations, the tidal amplitude or phase is poorly represented [*Muis et al.*, 2016]. Most of the underestimation of GTSR occurs in regions where surges are predominantly induced by tropical cyclones, while in extra-tropical regions the mean bias of GSTR is about 60% smaller. For DCESL, there is no clear difference in model performance in tropical areas (Table 1).

3.3. Limitations of the DCESL and GTSR Extremes

Several factors can explain the differences in performance of DCESL and GTSR. First, DCESL was developed when few global datasets were available and thus, the representation of both the tides and surges may have inaccuracies. For example, the observation datasets used for tidal harmonics and waves did not have a fully global coverage. Second, the model assumptions used to approximate extremes can have different effects that can lead to both an underestimation and overestimation. For example, the assumption of a straight coastline rather than the complex geometry of the coast could overestimate surge levels in some areas, and underestimate surge levels in other areas.

Two main assumptions result in an underestimation of surge levels. First, the use of daily averaged wind speed will smooth the peak winds, and hence, lower surge levels. Second, the assumption that storm surges always occur during mean high-tide level (H_{mh}) may lead to an overestimation, as it ignores the fact that storm surges also occur during low tide. We have verified the effect of the second assumption by using the GTSR time series for storm surges and tides. We calculated the mean high-tide level as the mean of the daily maximum of tidal levels over the period 1979–2014. Subsequently, we added the surge levels for

Table 1. Performance of DCESL and GTSR Extremes With Return Periods of 10, 100, and 1,000 Years (RP10, RP100, RP1000)

		DCESL			GTSR		
		RP10	RP100	RP1000	RP10	RP100	RP1000
Mean bias (m)[a]	Global	0.45 [0.51]	0.55 [0.56]	0.70 [0.63]	−0.15 [0.31]	−0.19 [0.37]	−0.21 [0.40]
	Extra-tropical	0.45 [0.52]	0.55 [0.56]	0.68 [0.60]	−0.10 [0.33]	−0.11 [0.36]	−0.12 [0.38]
	Tropical	0.46 [0.49]	0.55 [0.58]	0.72 [0.67]	−0.24 [0.27]***	−0.29 [0.35]***	−0.33 [0.40]***
Absolute error (m)[a]	Global	0.54 [0.41]	0.64 [0.46]	0.78 [0.52]	0.24 [0.26]	0.27 [0.31]	0.30 [0.34]
	Extra-tropical	0.55 [0.41]	0.64 [0.44]	0.77 [0.49]	0.21 [0.27]	0.23 [0.29]	0.25 [0.31]
	Tropical	0.53 [0.40]	0.64 [0.47]	0.80 [0.56]	0.27 [0.24]*	0.33 [0.32]**	0.37 [0.37]**
Hit rate (%)[b]	Global	8	19	26	15 [32]	21 [39]	23 [40]
	Extra-tropical	7	16	21	17 [33]	23 [40]	27 [43]
	Tropical	8	23	33	13 [32]	18 [37]	16 [37]

DCESL, DINAS-COAST Extreme Sea Levels; GTSR, Global Tide and Surge Reanalysis.
We show the absolute and relative differences between observed and modeled extreme sea levels. Values in brackets show the standard deviation. Only stations with more than 25 years of data are used. The results are separated for observation stations in extra-tropical and tropical regions (i.e., prone to tropical cyclones), each area has, respectively, 75 and 69 stations. The classification into extra-tropical and tropical is based on Note S2 and Figure S3 in *Muis et al.* [2016].
[a]The asterisks indicate whether the differences between extra-tropical and tropical areas are statistically significant for different levels of significance equal to ***$P < 0.01$, **$P < 0.05$, *$P < 0.1$. These significance levels are only calculated for the mean bias and absolute mean error.
[b]The values in the brackets show the hit rate for GTSR including the 5 and 95% confidence bounds of the fitted Gumbel distribution.

the same period, and recalculated the extreme sea levels. The DCESL assumption that storm surges occur during mean high-tide level leads to generally lower extremes than the original GTSR extremes. Hence, it actually leads to an underestimation of extremes. The mean error improves for only 21% of the observation stations (i.e., 30 out of 144). This suggests that the periodic occurrence of spring tides, which are smoothed by the use of mean high-tide level, is very important for the generation of extreme sea levels. An analysis of extreme sea-level data around the U.K. found a similar result [*Haigh et al.*, 2016].

The systematic overestimation of DCESL can also derive from the modeling assumptions used to compute the wind set-up. In particular, the assumption that the wind direction is perpendicular to the coast will lead to an overestimation of surge level as other wind directions may prevail and will lead to lower surge levels. Also, the assumption of an equilibrium for constant wind speed may overestimate the surge heights. Furthermore, the use wave observations may induce errors in several ways. For example, the translation from wave height to wind speed using an empirical relationship and a log-linear relationship to extrapolate the observed wave heights to longer return periods may have led to an overestimation of actual wind speeds, and subsequently the surge levels corresponding to specific return periods. Furthermore, waves may be generated elsewhere and then propagate. This can induce an overestimation of surge heights when translating those waves to wind speed for a particular location.

The bias of DCESL in regions prone to tropical cyclones is not significantly different from the bias in extra-tropical regions. However, the strong temporal and spatial gradients of tropical cyclones are unlikely to be adequately represented by the wave observations used to construct the wind set-up term. This is partly because tropical cyclones often destroy measurement devices [*Grinsted et al.*, 2012; *Torres and Tsimplis*, 2014]. Additionally, tropical cyclones are rare and affect only a small area, and therefore, observation records often do not contain a sufficient number of measurements [*Haigh et al.*, 2013]. Hence, while not apparent from the model performance, we can assume that surges induced by tropical cyclones are not fully represented by DCESL, but that this is masked by the general overestimation of DCESL.

The bias of GTSR in regions prone to tropical cyclones is significantly larger than the bias of GTSR in extra-tropical regions. This indicates that tropical cyclones in GTSR are under-represented. The relatively coarse spatial (~80 km) and temporal (6 h) resolution of the meteorological forcing data means that GTSM

10.1002/2016EF000430

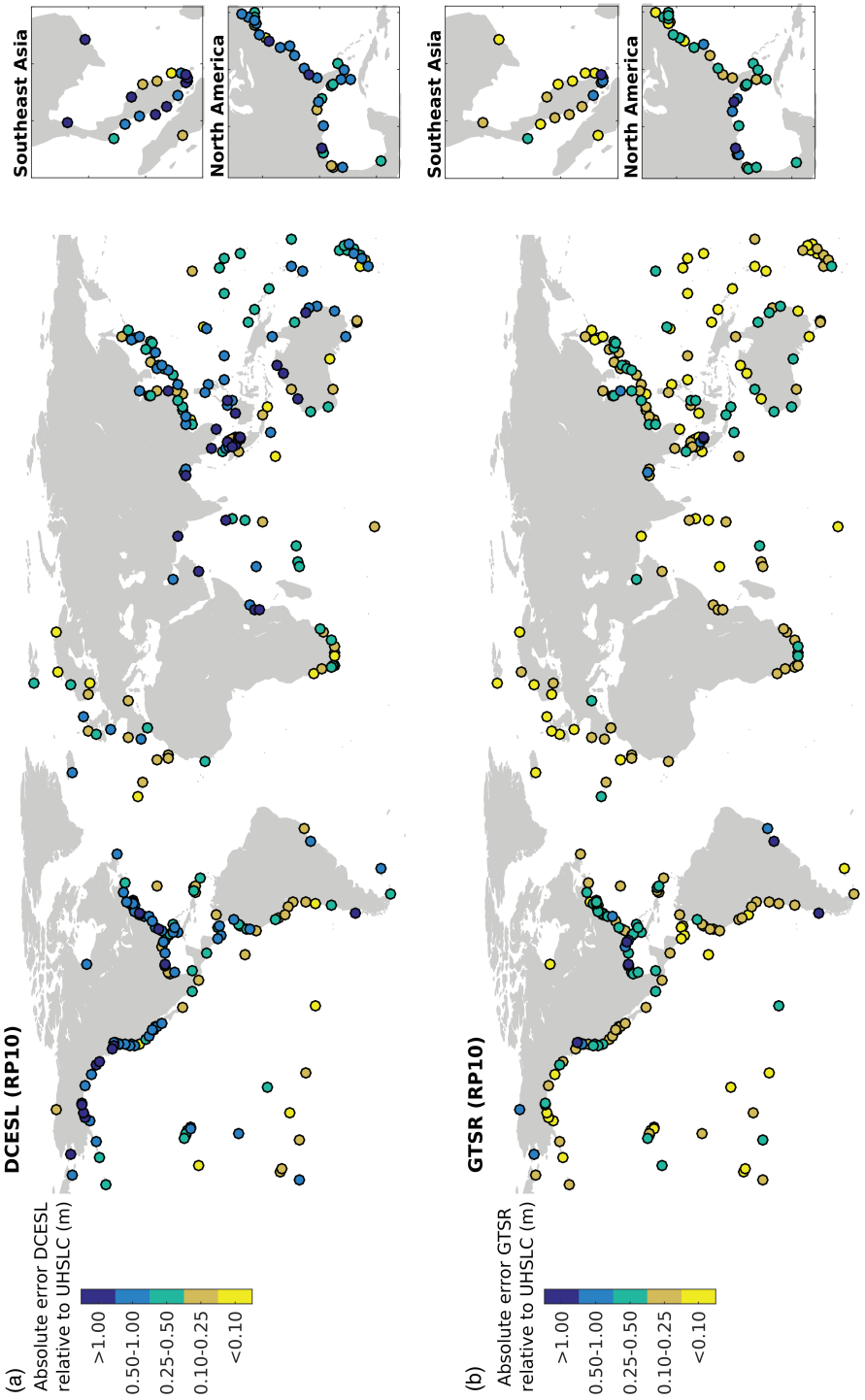

Figure 2. Maps showing the performance against observed extreme sea levels at the tide gauge locations: (a) the performance of DINAS-COAST Extreme Sea Levels (DCESL); and (b) the performance of Global Tide and Surge Reanalysis (GTSR) showed as the absolute error (m) between modeled and observed extreme sea levels with a return period of 10 years (RP10). We show the 280 out of the 472 observation stations that have more than 10 years of data and use the overlapping period from the modeled and observed sea levels for the extreme value statistics. The inset panels zoom in on Southeast Asia and the east coast of North America, since many locations overlap in those regions.

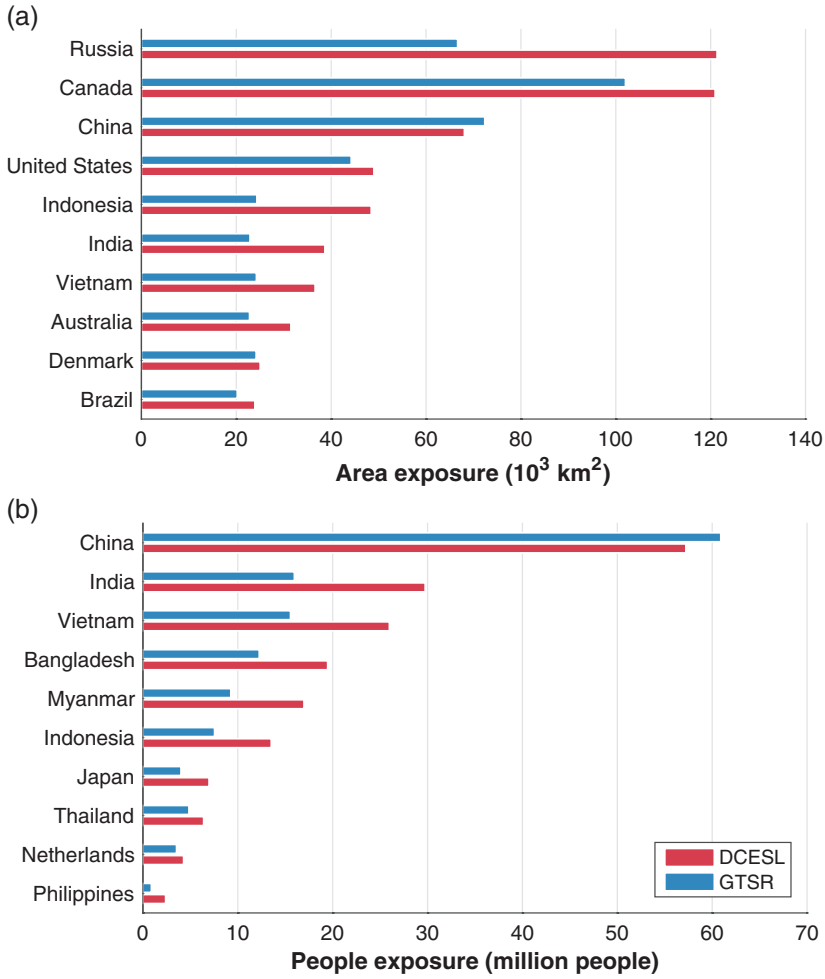

Figure 3. The top-10 ranked countries showing the countries with the highest: (a) exposed area, that is the area below the 1 in 100-year sea level; and (b) exposed population, that is the number of million people located below the 1 in 100-year sea level. The countries are ranked based on the DINAS-COAST Extreme Sea Levels (DCESL) estimates. Note that land area of Denmark includes Greenland.

inevitably fails to represent tropical cyclone-induced extremes, which are characterized by high spatial and temporal gradients. *Muis et al.* [2016] note other limitations that may contribute to the underestimation of GTSR, including the exclusion of baroclinic effects, tide–surge interactions, and the effect of precipitation and river discharge.

3.4. Flood Exposure Based on DCESL and GTSR

3.4.1. Comparison of Flood Exposure

Using the DIVA model, we calculated flood exposure in terms of the land area and the number of people below the 1 in 100-year sea levels. Figures 3a–3b shows the top 10 countries with the highest exposed area and the highest population exposed. Both DCESL and GTSR indicate that about 40% of the area exposed is located in Russia, Canada, and China. However, the global area exposed based on GTSR is 28% lower than the global area exposed based on DCESL. For about half of the countries that are exposed to coastal flooding, the area exposed is more than 40% lower when based on GTSR than when based on DCESL. The U.K. is an exception, where GTSR leads to a 31% increase in area exposed relative to the area exposed based on DCESL.

Similar to the exposed area, the global exposed population is 28% lower when based on GTSR instead of DCESL. Generally, GTSR leads to an increase in exposed population in northwest Europe and East Asia, and to a decrease in other parts of the world (Figure 4c). A large part of the exposed population is located in China, which accounts for 26 and 39% of the estimated global exposure for DCESL and GTSR, respectively. For six out of the top 10 countries with the largest exposed population, the estimated exposure is about

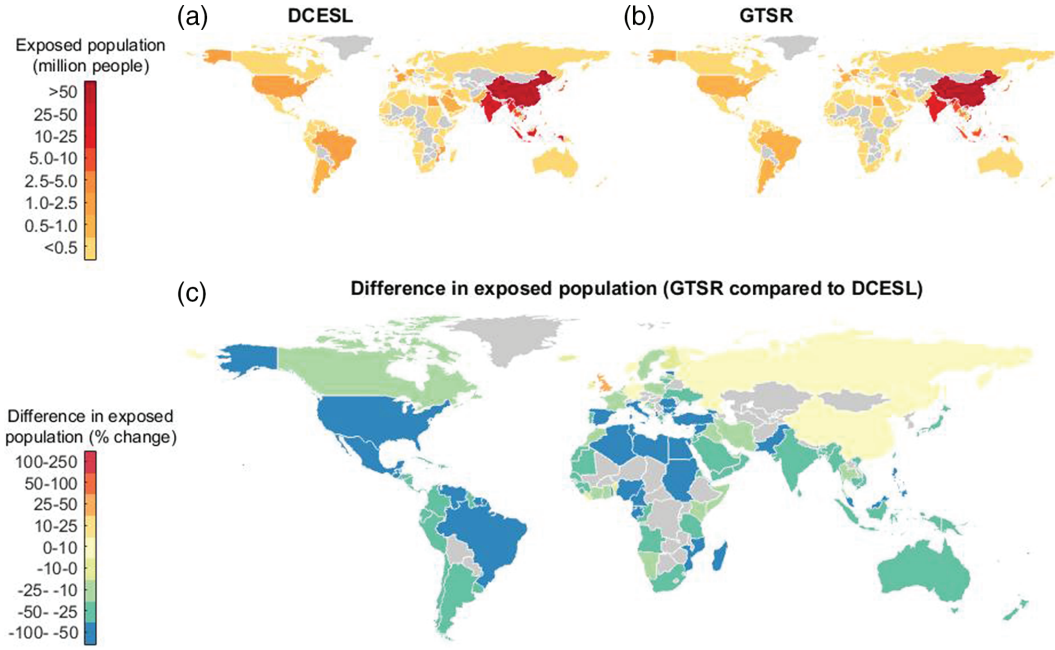

Figure 4. Comparison of exposed population to 1 in 100-year sea levels on a country-scale when based on, (a) DINAS-COAST Extreme Sea Levels (DCESL), and (b) Global Tide and Surge Reanalysis (GTSR), and (c) the difference between exposed population when based on DCESL and GTSR showed as the relative change compared to DCESL (%).

40–60% lower when based on GTSR than when based on DCESL (Figure 3a). Despite these large differences at the country scale, the global geographic pattern of exposed population for DCESL and GTSR is consistent (Figures 4a and 4b).

3.4.2. Effect of the Vertical Datum Correction

Previous studies at continental to global-scale have not accounted for the fact that GTSR and DCESL are referenced to mean sea level [*Jongman et al.*, 2012; *Hinkel et al.*, 2014; *Muis et al.*, 2016], whereas global elevation datasets, such as SRTM, are referenced to the EGM96 geoid. Correcting the vertical datum has a large effect on estimated flood exposure (Table 2). Globally, the correction of the vertical datum results in an increase of 16 and 20% in exposed land area for DCESL and GTSR, respectively. The correction has an even larger effect on the exposed population, which increases with 39 and 60% for DCESL and GTSR, respectively. Figure S4 shows the changes in exposed population due to the correction in vertical datum for the 1 in 100-year GTSR extremes. The large changes are explained by the large values of the MDT in East Asia (Figure S1), which is low-lying and densely populated. For example in Indonesia (MDT ranges from 0.8 to 1.1 m) exposed population more than doubles due to the correction. In contrast, in France (MDT ranges from −0.1 to 0 m) the correction results in minor decrease (<10%) in exposed population. This is also demonstrated in Figure 5, which maps the inundation for the 1 in 100-year extremes before and after the vertical datum correction for the Thames estuary and the Bay of Bengal. This shows that there are minor effects in the Thames estuary, but much larger effects in the northern Bay of Bengal; the latter results in a large increase in area and population exposed in West Bengal and Bangladesh. The effects of the correction of the vertical datum are much larger than the effects of using either the DCESL or GTSR extremes. Our results demonstrate that for impact modeling, it is essential to ensure that the extreme sea levels and land elevation dataset are referenced to the same vertical datum.

3.5. Challenges for Impact Modeling

We demonstrated that a dynamical approach and accounting for vertical datum differences provides an improved basis for the assessment of coastal flood impacts. However, various challenges remain with regard to the data and methods that are used for these types of assessments. One important challenge is to improve inundation modeling at the global-scale, which is now limited to planar "bath-tub" inundation models. These models generally overestimate the flood extent [*Ramirez et al.*, 2016]. The uncertainty in global elevation data also limits the accuracy of the global modeling of coastal impacts [*Schumannm*,

Table 2. The Effect of the Correction in Vertical Datum on Flood Exposure for DCESL and GTSR

	Uncorrected (Referenced to Mean Sea Level)	Corrected (Referenced to EGM96 Geoid)
Exposed area (10^3 km^2)		
DCESL	647	770
GTSR	446	555
Exposed population (million people)		
DCESL	157	218
GTSR	99	158

DCESL, DINAS-COAST Extreme Sea Levels; GTSR, Global Tide and Surge Reanalysis.
Flood exposure is expressed as the exposed area, i.e., the area below the 1 in 100-year sea levels, and the exposed population, the number of people below the 1 in 100-year sea levels.

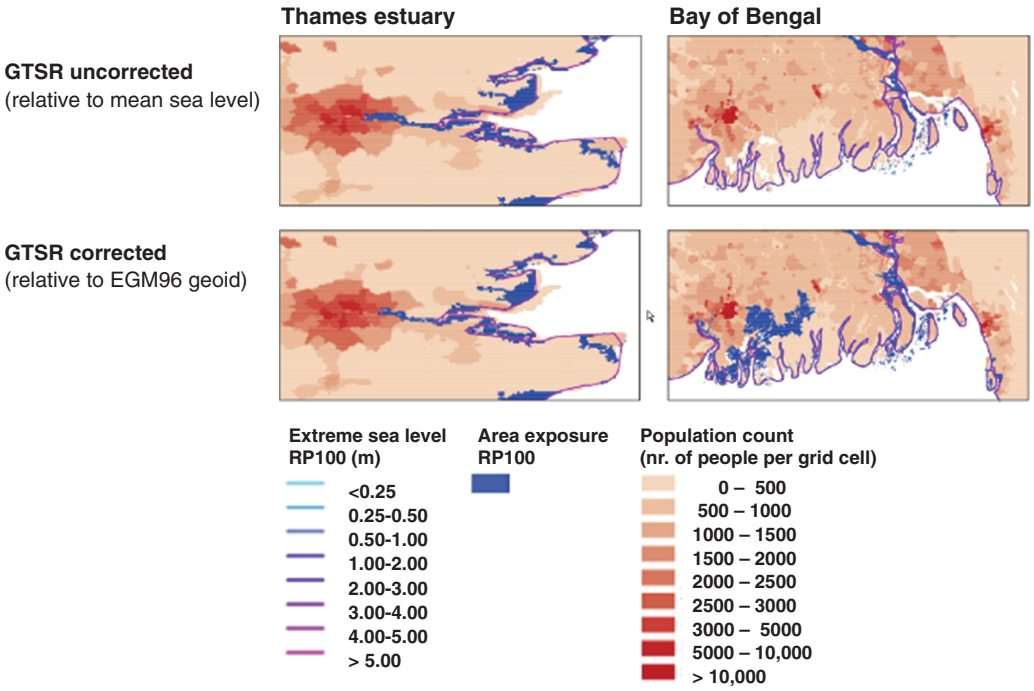

Figure 5. Potential inundation maps, including population exposure, for the 1 in 100-year sea levels for two known coastal flood hotspots. The left panels show the Thames estuary and the right panels show the northern Bay of Bengal. The upper panels show the results before correcting the vertical datum of Global Tide and Surge Reanalysis (GTSR), i.e., extreme sea levels referenced to mean sea level. The bottom panels shows the results after correcting GTSR for the vertical datum, i.e., extreme sea level referenced to EGM96 geoid. We consider coastal flooding only and no flood protection. The maps are based on a simple bath-tub inundation model [*Muis et al.*, 2016].

2014], in part caused by the presence of vegetation and other elements causing offsets in the terrain. *Hinkel et al.* [2014] and *Lichter et al.* [2011] found differences up to 75–150% in inundated area estimates when using different elevation datasets. Similarly, *Wolff et al.* [2016] found that the use of one elevation model over another can result in differences up to 50% in flood damages.

Figure 5 maps the potential inundation extent of the 1 in 100-year sea levels for the northern Bay of Bengal. It shows that GTSR results in limited coastal flooding of West Bengal and Bangladesh, even after correcting the vertical datum. Considering that Bangladesh has experienced many major flooding events in the last century with hundreds of thousands of deaths [*Flierl and Robinson*, 1972; *Ali*, 1999; *Alam and Dominey-Howes*, 2015], this indicates that GTSR underestimates the flood hazard. The underestimation of the flood exposure can be explained by: (1) the quality of the SRTM elevation model, which may overestimate the elevations in the coastal zone [*Kulp and Strauss*, 2016]; (2) not accounting for interactions between

coastal extremes and river flows; and (3) the underrepresentation of tropical cyclones in the GTSR dataset. For example, in Bangladesh, the 1 in 100-year sea levels are estimated as 5.5 and 4.1 m for DCESL and GTSR, respectively, while over the last 55 years there have been 15 tropical cyclones that induced extremes with a height ranging from 2.5 to 10.6 m [*Karim and Mimura*, 2008]. In regions they affect, tropical cyclones are often the most damaging storms [*Woodruff et al.*, 2013]. As such, to improve the global modeling of coastal flooding it is essential that future studies focus on the improvement of storm surges induced by tropical cyclones.

3.6. Developments and Use of Global-Scale Assessments of Coastal Flood Risk

There have been various attempts to assess coastal risks at the global-scale. The main goal of these assessments has been to identify risk hotspots in a world with rising sea levels. One of the first global assessments was the Worldwide Cost Estimate [*Rijkswaterstaat and Delft Hydraulics*, 1990], conducted to inform the First Assessment Report of the *Intergovernmental Panel on Climate Change (IPCC)* [1990]. They estimated that the total protection costs against permanent submergence for 1 m of sea-level rise were in the order of 500 billion 1990 USD or 0.4% of the global gross domestic product at that time. The GVA [*Hoozemans et al.*, 1992, 1993; *Nicholls and Hoozemans*, 2005] extended the global analysis to include national estimates of extreme sea levels and defense standards. They estimated that 200–250 million people per year (4–5% of the global population in 1990) were exposed to coastal flooding (i.e., lived below the 1 in 1,000-year extreme sea level). A 1-m rise of mean sea level increased this exposure by 50% without any other changes. This formed a foundation of studies that considered realistic sets of sea-level rise/subsidence and socio-economic change scenarios, demonstrating the flood impacts of sea-level rise, in the context of other change, including adaptation [*Nicholls et al.*, 1999; *Nicholls*, 2004]. Most recently, applying the DCESL extremes, *Hinkel et al.* [2014] estimated that 0.01–0.02 % of the global population in 1990 (i.e., 0.8–1.1 million people) experience coastal flooding on average per year. Without adaptation, 25–123 cm of global mean sea-level rise by 2100 will result in 0.2–4.6% of the world population experiencing coastal flooding on average per year. Due to the use of different definitions, approaches, and scenarios, it is not possible to directly compare the results from the different studies. However, these and other studies show a clear advance of the global models over time. They have provided important insights into the dynamics of coastal flood risk, including regional trends.

In future studies, the GTSR extremes can be used to assess the damages of coastal flooding under a range of sea-level rise and socio-economic scenarios, and including assumptions about adaptation and protection, following *Hinkel et al.* [2014]. The use of a dynamical approach enables the possibility to assess how changes in the frequency and intensity of storm may affect the occurrence of coastal floods. Previous studies at the local and at European scale have forced hydrodynamic models with outputs from climate model ensembles for different future projections to assess changes in storm surge due to a changing climate [e.g., *Vousdoukas et al.*, 2016]. In general, the use of a hydrodynamic approach allows to extend the simulation beyond the observed period. Although the meteorological dataset before 1979 have larger uncertainties, extending the simulation period would reduce the uncertainty in the extreme values statistics. For example, the 20th Century Reanalysis (1871–2010) dataset has been demonstrated to be very valuable for the analysis of historical storm surges [*Dangendorf et al.*, 2014; *Cid et al.*, 2017]. Another research direction may be to use multi-member global climate model ensembles or seasonal forecast ensemble runs. For example, the archived runs of the European Centre for Medium-Range Weather Forecasts (ECMWF) provide independent sets of over 1,500 years for regions where the forecasts have little seasonal skill. This set can be used to decrease the statistical uncertainty in extreme sea levels [*van den Brink et al.*, 2004].

Global flood risk models are being used increasingly by practitioners and decision-makers to, for example, rapidly assess risk in data-scarce countries [*Ward et al.*, 2015]. This is also the case for the GTSR dataset, which is accessible via different web-based tools. One of these tools is ThinkHazard! (www.thinkhazard.org). ThinkHazard! is developed by the Global Facility for Disaster Reduction and Recovery (GFDRR) enables people to discover the level of hazard in any location around the world. Another tool where GTSR will be implemented is the Aqueduct Global Flood Analyzer developed by the World Resources Institute (www.wri.org/floods). Aqueduct maps water risk around the world to help companies, investors, policy-makers, and other users to understand how water risk are emerging around the world. Aqueduct Global Flood Analyzer 2.0 will be launched in 2017 and will include estimates of exposed population, exposed Gross Domestic Product (GDP) and urban damages for a wide range of sea-level rise projections and socio-economic scenarios. This tool

has the functionality to allow users to assess how much risk could be avoided if flood protection standards were increased by building dikes or levees. Assessing the effectiveness of those strategies under future climate conditions can support decisions on climate change mitigation and adaptation [*Ward et al.*, 2015].

4. Conclusions

The intercomparison of DCESL and GTSR showed that there are large differences between the two datasets and that these differences are generally larger than the confidence intervals of GTSR. However, the geographic patterns of extreme sea levels of the two datasets are in qualitative agreement. Evaluating the performance of DCESL and GTSR against observed extremes showed that, whereas the DCESL extremes are generally overestimated, the GTSR extremes are generally underestimated, particularly in the tropics. Compared to observations, the bias of GTSR is about 70% smaller than the bias of DCESL.

Using the DIVA model, we assessed flood exposure based on 1 in 100-year sea-level extremes for present-day conditions (i.e., the year 2015). Both the exposed area and exposed population are both 28% lower when based on GTSR than when based on DCESL. We emphasize that for inundation modeling it is essential to use the correct vertical datum. Past studies that estimate flood exposure at the continental- to global-scale have often used sea-level extremes referenced to mean sea level, rather than the geoid used by the elevation datasets. This induces large errors and greatly affects flood exposure. Globally, the correction in vertical datum results in an increase of exposed area and exposed population of, respectively, 16 and 39% for DCESL, and 20 and 60% for GTSR. Effects are even larger in regions where there is a large offset in mean sea level and the EGM96 geoid, such as East Asia.

To conclude, we demonstrated that a hydrodynamic approach and a correction of the vertical datum provides an improved basis for the assessment of coastal flood impacts. In future research, GTSR can be used to assess flood risk both for present-day climate and under future climate and socio-economic scenarios, including confidence intervals. Further advancement in coastal flood assessments may come from the improvement of the representation of tropical cyclones, including flood dynamics in large-scale inundation modeling, and, the availability of higher accuracy global elevation products.

Acknowledgments
The 1-in-100-year extreme sea levels of the GTSR dataset are freely available online at the archive of the 4TU.Research Data on doi:10.4121/uuid:aa4a6ad5-e92c-468e-841b-de07f7133786. Other parts of the GTSR dataset may be available upon request. The observations from tide gauge stations were obtained from UHSCL dataset are freely available online (http://uhslc.soest.hawaii.edu/). The SRTM data are made available by CGIAR-CSI (http:/srtm.csi.cgiar.org). The GRUMP data are available from the Socioeconomic Data and Applications Center (http://sedac.ciesin.columbia.edu/) following registration. The MDT data were obtained freely from AVISO (http://www.aviso.altimetry.fr). S.M., R.J.N., S.B., J.H., D.L., A.T.V., P.S., H.C.W., and P.J.W. were funded by the European research project RISES-AM (grant agreement 603396). P.J.W. received additional funding from the Nederlandse Organisatie voor Wetenschappelijk Onderzoek (NWO) in the form of a VIDI grant (grant 016.161.324). J.H. and D.L. have also received funding from the European Union's Horizon 2020 research and innovation programme under grant agreement 642018 (GREEN-WIN project). The research leading to these results also received funding from the Aqueduct Global Flood Analyzer project, via subsidy 5000002722 from the Netherlands Ministry of Infrastructure and the Environment. The project is convened by the World Resources Institute. We thank Claudia Wolff for her assistance with the DIVA simulations. The authors also thank Thomas Wahl and two anonymous reviewers for their helpful comments and suggestions.

References

Alam, E., and D. Dominey-Howes (2015), A new catalogue of tropical cyclones of the northern Bay of Bengal and the distribution and effects of selected landfalling events in Bangladesh, *Int. J. Climatol.*, *35*(6), 801–835. doi:10.1002/joc.4035.

Ali, A. (1999), Climate change impacts and adaptation assessment in Bangladesh, *Clim. Res.*, *12*, 109–116. doi:10.3354/cr012109.

van den Brink, H. W., G. P. Können, J. D. Opsteegh, G. J. van Oldenborgh, and G. Burgers (2004), Improving 10^4-year surge level estimates using data of the ECMWF seasonal prediction system, *Geophys. Res. Lett.*, *31*(17), 1–4. doi:10.1029/2004GL020610.

Brown, S., R. J. Nicholls, J. A. Lowe, and J. Hinkel (2013), Spatial variations of sea-level rise and impacts: An application of DIVA, *Clim. Change*, *134*(3), 403–416. doi:10.1007/s10584-013-0925-y.

Carrere, L., F. Lyard, M. Cancet, A. Guillot, and L. Roblou (2012), FES 2012: A new global tidal model taking advantage of nearly 20 years of altimetry, in *20 Years of Progress in Radar Altimetry* , pp. 6 , ESA/CNES, Venice, Italy.

Center for International Earth Science Information Network (CIESIN), Columbia University International Food Policy Research Institute (IFPRI), The World Bank, and Centro Internacional de Agricultura Tropical (CIAT) (2011), *Global Rural–Urban Mapping Project, Version 1 (GRUMPv1): Population Count Grid*. Palisades, NY: NASA Socioeconomic Data and Applications Center (SEDAC). doi:10.7927/H4GH9FVG.

Cid, A., P. Camus, S. Castanedo, F. J. Méndez, and R. Medina (2017), Global reconstructed daily surge levels from the 20th Century Reanalysis (1871–2010), *Global Planet. Change*, *148*(2017), 9–21. doi:10.1016/j.gloplacha.2016.11.006.

Dangendorf, S., S. Müller-Navarra, J. Jensen, F. Schenk, T. Wahl, and R. Weisse (2014), North Sea storminess from a novel storm surge record since AD 1843, *J. Clim.*, *27*(10), 3582–3595. doi:10.1175/jcli-d-13-00427.1.

Dee, D. P., et al. (2011), The ERA-Interim reanalysis: Configuration and performance of the data assimilation system, *Q. J. Roy. Meteorol. Soc.*, *137*(656), 553–597. doi:10.1002/qj.828.

Farr, T., and M. Kobrick (2001), The shuttle radar topography mission, *Rev. Geophys.*, *82*(2005), 47. doi:10.1029/2005rg000183.

Flierl, G. R., and A. R. Robinson (1972), Deadly surge in the Bay of Bengal – Dynamics and storm-tide tables, *Nature*, *239*, 213–215. doi:10.1038/239213a0.

Grinsted, A., J. C. Moore, and S. Jevrejeva (2012), Homogeneous record of Atlantic hurricane surge threat since 1923, *Proc. Natl. Acad. Sci. U. S. A.*, *109*(48), 19601–19605. doi:10.1073/pnas.1209542109.

Gumbel, E. J. (1941), The return period of flood flows, *Ann. Math. Stat.*, *12*(2), 163–190. doi:10.1214/aoms/1177731747.

Güneralp, B., İ. Güneralp, and Y. Liu (2015), Changing global patterns of urban exposure to flood and drought hazards, *Global Environ. Change*, *31*, 217–225. doi:10.1016/j.gloenvcha.2015.01.002.

Haigh, I. D., E. M. S. Wijeratne, L. R. MacPherson, C. B. Pattiaratchi, M. S. Mason, R. P. Crompton, and S. George (2013), Estimating present day extreme water level exceedance probabilities around the coastline of Australia: Tides, extra-tropical storm surges and mean sea level, *Clim. Dyn.*, *42*(1–2), 121–138. doi:10.1007/s00382-012-1652-1.

Haigh, I. D., M. P. Wadey, T. Wahl, O. Ozsoy, R. J. Nicholls, J. M. Brown, K. J. Horsburgh, and B. Gouldby (2016), Analysis: Spatial and temporal analysis of extreme sea level and storm surge events around the coastline of the UK, *Sci. Data*, *3*(160107), 1–14. doi:10.1038/sdata.2016.107.

Hallegatte, S., C. Green, R. J. Nicholls, and J. Corfee-Morlot (2013), Future flood losses in major coastal cities, *Nat. Clim. Change*, *3*(9), 802–806. doi:10.1038/nclimate1979.
Hinkel, J., and R. J. T. Klein (2009), Integrating knowledge to assess coastal vulnerability to sea-level rise: The development of the DIVA tool, *Global Environ. Change*, *19*(3), 384–395. doi:10.1016/j.gloenvcha.2009.03.002.
Hinkel, J., S. Brown, L. Exner, R. J. Nicholls, A. T. Vafeidis, and A. S. Kebede (2011), Sea-level rise impacts on Africa and the effects of mitigation and adaptation: An application of DIVA, *Reg. Environ. Change*, *12*(1), 207–224. doi:10.1007/s10113-011-0249-2.
Hinkel, J., D. Lincke, A. T. Vafeidis, M. Perrette, R. J. Nicholls, R. S. J. Tol, B. Marzeion, X. Fettweis, C. Ionescu, and A. Levermann (2014), Coastal flood damage and adaptation costs under 21st century sea-level rise, *Proc. Natl. Acad. Sci. U. S. A.*, *111*(9), 3292–3297. doi:10.1073/pnas.1222469111.
Hogben, N., N. M. C. Dacunha, and K. S. Andrews (1986), *Global Wave Statistics*, Unwin Brothers, London, U. K..
Hoozemans, F. M. J., M. Marchand, H. A. Pennekamp, M. Stive, R. Misdorp, and L. Bijlsma (1992), The impacts of sea-level rise on coastal areas: Some global results, in *The Rising Challenge of the Sea* , pp. 275–292 , NOAA, Margarita Island, Venzuela.
Hoozemans, F. M. J., M. Marchand, and H. A. Pennekamp (1993), *Sea Level Rise: A Global Vulnerability Assessment (GVA) – Vulnerability Assessment for Population, Coastal Wetlands and Rice Production on a Global Scale* Second Rev, Delft Hydraulics and Rijkswaterstaat; The Hague, Delft, The Netherlands.
Hurdle, D. P., and R. J. H. Stive (1989), *Revision of SPM 1984 Wave Hindcast Model to Avoid Inconsistencies in Engineering Application*, Elsevier, Amsterdam, The Netherlands.
Intergovernmental Panel on Climate Change (IPCC) (1990), *The IPCC Scientific Assessment Report – Working Group 1*, Climate Change: The IPCC Scientific Assessment, Cambridge Univ. Press Cambridge, U. K., *24*, 263. doi:10.2307/1551672.
Jarvis, A., H. I. I. Reuter, A. Nelson, and E. Guevara (2008), *Hole-filled seamless SRTM data V4*, Int. Cent. Trop. Agric. [Available at http://srtm.csi.cgiar.org.]
Jongman, B., P. J. Ward, and J. C. J. H. Aerts (2012), Global exposure to river and coastal flooding: Long term trends and changes, *Global Environ. Change*, *22*(4), 823–835. doi:10.1016/j.gloenvcha.2012.07.004.
Karim, M., and N. Mimura (2008), Impacts of climate change and sea-level rise on cyclonic storm surge floods in Bangladesh, *Global Environ. Change*, *18*(3), 490–500. doi:10.1016/j.gloenvcha.2008.05.002.
Kron, W. (2013), Coasts: The high-risk areas of the world, *Nat. Hazards*, *66*(2013), 1363–1382. doi:10.1007/s11069-012-0215-4.
Kulp, S., and B. H. Strauss (2016), Global DEM errors underpredict coastal vulnerability to sea level rise and flooding, *Front. Earth Sci.*, *4*, 1–8. doi:10.3389/feart.2016.00036.
Lichter, M., A. T. Vafeidis, R. J. Nicholls, and G. Kaiser (2011), Exploring data-related uncertainties in analyses of land area and population in the "Low-Elevation Coastal Zone" (LECZ), *J. Coast. Res.*, *274*(4), 757–768. doi:10.2112/jcoastres-d-10-00072.1.
Maxwell, B. A., and R. W. Buddemeier (2002), Coastal typology development with heterogeneous data sets, *J. Mater. Cycles Waste Manage.*, *3*(1–3), 77–87. doi:10.1007/s10113-001-0034-8.
McFadden, L., R. J. Nicholls, A. T. Vafeidis, and R. S. J. Tol (2007), A methodology for modeling coastal space for global assessment, *J. Coast. Res.*, *234*, 911–920. doi:10.2112/04-0365.1.
Muis, S., B. Güneralp, B. Jongman, J. C. J. H. Aerts, and P. J. Ward (2015), Flood risk and adaptation strategies under climate change and urban expansion: A probabilistic analysis using global data, *Sci. Total Environ.*, *538*, 445–457. doi:10.1016/j.scitotenv.2015.08.068.
Muis, S., M. Verlaan, H. C. Winsemius, J. C. J. H. Aerts, and P. J. Ward (2016), A global reanalysis of storm surge and extreme sea levels, *Nat. Commun.*, *7*(11969), 1–11. doi:10.1038/ncomms11969.
National Geophysical Data Center (NGDC) (2001), *CDROM, ETOPO2 Global 2' Elevations.*
Nicholls, R. J. (2004), Coastal flooding and wetland loss in the 21st century: Changes under the SRES climate and socio-economic scenarios, *Global Environ. Change*, *14*(1), 69–86. doi:10.1016/j.gloenvcha.2003.10.007.
Nicholls, R. J., and A. Cazenave (2010), Sea-level rise and its impact on coastal zones, *Science*, *328*, 1517–1520. doi:10.1126/science.1185782.
Nicholls, R. J., and F. M. J. Hoozemans (2005), Global vulnerability analysis, in *Encyclopedia of Coastal Science*, edited by M. Schwartz , pp. 486–491 , Kluwer Acad. Publ., Dordrecht, The Netherlands.
Nicholls, R. J., F. M. J. Hoozemans, and M. Marchand (1999), Increasing flood risk and wetland losses due to global sea-level rise: Regional and global analyses, *Global Environ. Change*, *9*, S69–S87. doi:10.1016/S0959-3780(99)00019-9.
Nicholls, R. J., S. Brown, S. E. Hanson, and J. Hinkel (2010), *Economics of coastal zone*: *Adaptation to climate change*, Development and Climate Change Discussion Paper, Washington D.C.
Ramirez, J. A., M. Lichter, T. J. Coulthard, and C. Skinner (2016), Hyper-resolution mapping of regional storm surge and tide flooding: Comparison of static and dynamic models, *Nat. Hazards*, *82*(1), 571–590. doi:10.1007/s11069-016-2198-z.
Rijkswaterstaat, and Delft Hydraulics (1990), *Sea Level Rise: A Worldwide Cost Estimate of Basic Coastal Defense Measures*, CZM Workshop, Perth, Australia.
Rio, M. H., S. Mulet, and N. Picot (2014), Beyond GOCE for the ocean circulation estimate: Synergetic use of altimetry, gravimetry, and in situ data provides new insight into geostrophic and Ekman currents, *Geophys. Res. Lett.*, *41*(24), 8918–8925. doi:10.1002/2014GL061773.
Schaeffer, P., Y. Faugére, J. F. Legeais, A. Ollivier, T. Guinle, and N. Picot (2012), The CNES_CLS11 global mean sea surface computed from 16 years of satellite altimeter data, *Mar. Geod.*, *35*(Suppl. 1), 3–19. doi:10.1080/01490419.2012.718231.
Schumannm, G. J. P. (2014), Fight floods on a global scale, *Nature*, *507*(7491), 169. doi:10.1038/507169e.
Sugiyama, M., R. J. Nicholls, and A. T. Vafeidis (2008), *Estimating the Economic Cost of Sea-Level Rise*, MIT Global Change Joint Prog. Publ., Cambridge, Mass.
Torres, R. R., and M. N. Tsimplis (2014), Sea level extremes in the Caribbean Sea, *J. Geophys. Res. Ocean*, *119*, 4714–4731. doi:10.1002/2014JC009929.
Vafeidis, A. T., R. J. Nicholls, L. McFadden, R. S. J. Tol, J. Hinkel, T. Spencer, P. S. Grashoff, G. Boot, and R. J. T. Klein (2008), A new global coastal database for impact and vulnerability analysis to sea-level rise, *J. Coast. Res.*, *244*, 917–924. doi:10.2112/06-0725.1.
Verlaan, M., S. De Kleermaeker, and L. Buckman (2015), GLOSSIS: Global storm surge forecasting and information system, in *Australasian Coasts & Ports Conference 2015*, pp. 1–6, Auckland, New Zealand.
Vousdoukas, M. I., E. Voukouvalas, A. Annunziato, A. Giardino, and L. Feyen (2016), Projections of extreme storm surge levels along Europe, *Clim. Dyn.*, *47*(9), 1–20. doi:10.1007/s00382-016-3019-5.
Ward, P. J., M. A. Marfai, F. Yulianto, D. R. Hizbaron, and J. C. J. H. Aerts (2010), Coastal inundation and damage exposure estimation: A case study for Jakarta, *Nat. Hazards*, *56*(3), 899–916. doi:10.1007/s11069-010-9599-1.
Ward, P. J., et al. (2015), Usefulness and limitations of global flood risk models, *Nat. Clim. Change*, *5*(8), 712–715. doi:10.1038/nclimate2742.

Weenink, M. P. H. (1958), *A Theory and Method of Calculation of Wind Effects on Sea Levels in a Partly Enclosed Sea With Special Application to the Southern Coast of the North Sea*, KNMI, Staatsdrukkerij- en uitgeverijbedrijf, 's-Gravenhage.
Wolff, C., A. T. Vafeidis, D. Lincke, C. Marasmi, and J. Hinkel (2016), Effects of scale and input data on assessing the future impacts of coastal flooding: An application of DIVA for the Emilia-Romagna Coast, *Front. Mar. Sci.*, *3*, 1–15. doi:10.3389/fmars.2016.00041.
Woodruff, J. D., J. L. Irish, and S. J. Camargo (2013), Coastal flooding by tropical cyclones and sea-level rise, *Nature*, *504*(7478), 44–52. doi:10.1038/nature12855.